British Journal of Pharmaceutical Research

16(6): 1-11, 2017; Article no.BJPR.33212
ISSN: 2231-2919, NLM ID: 101631759

Thermodynamic Analysis for Adsorption of Amoxicillin onto Magnetic Carbon Nanotubes

Davoud Balarak[1], Ferdos Kord Mostafapour[1] and Ali Joghtaei[2*]

[1]Department of Environmental Health, Health Promotion Research Center, School of Public Health, Zahedan University of Medical Sciences, Zahedan, Iran.
[2]Student Research Committee, Qom University of Medical Sciences, Qom, Iran.

Authors' contributions

This work was carried out in collaboration between all authors. All authors read and approved the final manuscript.

Article Information

DOI: 10.9734/BJPR/2017/33212
Editor(s):
(1) Wenbin Zeng, School of Pharmaceutical Sciences, Central South University, Hunan, China.
Reviewers:
(1) Tom Rybolt, University of Tennessee at Chattanooga, USA.
(2) David K. Mills, Louisiana Tech University, USA.
(3) Fleming Martinez, National University of Colombia, Colombia.
(4) Tabinda Sattar, Bahaudin Zakaraya University, Multan, Pakistan.
Complete Peer review History: http://www.sciencedomain.org/review-history/19219

Original Research Article

Received 4th April 2017
Accepted 12th May 2017
Published 27th May 2017

ABSTRACT

The effect of temperature on the equilibrium adsorption of Amoxicillin (AMO) from aqueous solution using modified magnetic multi-walled carbon nanotubes ($MMWCNT_S$) was investigated. The equilibrium adsorption data were analyzed using three widely applied isotherms: Langmuir, Freundlich and Tempkin. The results revealed that Langmuir isotherm fit the experimental results well. Kinetic analyses were conducted using pseudo-first and second-order models and the intraparticle diffusion model. The regression results showed that the adsorption kinetics were more accurately represented by pseudo-second-order model. Standard free energy changes (ΔG^0), standard enthalpy change (ΔH^0), and standard entropy change (ΔS^0) were calculated at different temperatures. The ΔG^0 values were negative and ΔH^0 values and ΔS^0 values of $MMWCNT_S$ were positive; and suggested that the AMO adsorption on $MMWCNT_S$ was a spontaneous and endothermic process.

Keywords: Adsorption; $MMWCNT_S$; isotherm; amoxicillin; thermodynamics.

**Corresponding author: Email: alijoghatayi69@gmail.com;*

1. INTRODUCTION

The last two decades have witnessed the widespread emergence of pharmaceuticals in environmental matrices, i.e. surface water, groundwater, soils and sediments [1,2]. Among the various pharmaceutical compounds, antibiotics have been received particular attention because of their potential role in the development of antibiotic-resistant bacteria [3,4]. Antibiotics are used extensively in human and veterinary medicine, as well as in aquaculture to prevent or treat microbial infections. Most antibiotics tested to date are known to be bio-recalcitrant under aerobic conditions [5,6].

The presence of antibiotics in the aquatic environment has created two issues [7]. The immediate concern is the potential toxicity to aquatic organisms, and also to humans through drinking water [8 9]. In addition, there is growing alarm that release of antibiotics to the environment contributes to the emergence of strains of disease-causing bacteria, resistant to high doses of these drugs [10,11].

Amoxicillin (AMO) is a drug belonging to the class of β-lactam antibiotics that has a broad spectrum against both Gram-negative and Gram-positive bacteria [12]. AMO is one of the top-priority human and veterinary pharmaceuticals, and should receive greater attention in the management of environmental systems in all countries due to its high consumption [13,14].

Current data available in the literature indicate that conventional treatment methods used in water treatment (coagulation, flocculation, sedimentation, sand filtration, and disinfection with chlorine) and wastewater treatment (primary settling, activated sludge or trickling filter, and secondary settling) are not effective for removal of all pharmaceuticals present in raw water and wastewater [15-18]. This is because pharmaceuticals differ greatly in structure and in their physical and chemical properties which affect their rate of removal during treatment [19,20].

Among these methods, the adsorption method has the advantage of easy operation, low cost, high efficiency, and no risk of highly toxic byproducts; It is considered one of the most promising technologies [21,22]. Adsorption of amoxicillin on chitosan beads has been reported, where the kinetics and equilibrium of amoxicillin adsorption on chitosan fitted well to the Langmuir type [23]. Recently, adsorption of antibiotics onto activated carbon has been investigated, and results show that the adsorption of amoxicillin onto activated carbon plays an important role [24,25]. However, the most used adsorbents in this process are activated carbons (GACs) which are costly [26]. Consequently, there is much interest in finding alternative adsorbents that are inexpensive to implement.

A carbon nanotube (CNTs), as new adsorbent has gained increasing attention by many researchers. According to the grapheme layer, CNTs can be classified into single-wall CNTs (SCNTs) and multi-wall CNTs (MWCNTs) [27,28]. Due to their large specific surface area, small size, and hollow and layered structures, CNTs have been proven to possess great potential as superior adsorbents for removing many kinds of organic and inorganic contaminants [29,30].

Magnetic separation technology has been gradually attracting the attention of many scientists and technicians as a rapid and effective technology for separating magnetic materials. Magnetic separation technology combined with adsorption on adsorbent has been widely used in environmental purification applications. The introduction of magnetic properties into multi-wall carbon nanotubes system will combine the high adsorption capacity of CNTs and the separation convenience of magnetic materials [31,32]. In this study, multi-walled carbon nanotubes modified with magnetic nanoparticles were used for removal of AMO from wastewater samples. The adsorption isotherms of the AMO into adsorbent were investigated.

2. MATERIALS AND METHODS

2.1 Reagents and Materials

All chemicals were of analytical reagent grade or the highest purity available from Merck (Darmstadt, Germany) and double distilled water was used throughout the study.

In addition, all glassware were soaked in dilute nitric acid for 12 h and finally rinsed three times with double distilled water prior to use. Fig. 1 shows the structure of the investigated AMO. Stock solutions of AMO were prepared by dissolving the powder in double distilled water. AMO solutions of different initial concentrations were prepared by diluting the stock solution in appropriate proportions.

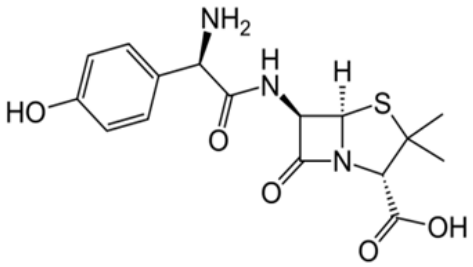

Fig. 1. Molecular structure of Amoxicillin (AMO)

2.2 Synthesis of Magnetic-Modified Multi-Walled Carbon Nano Tubes

Multi-wall carbon nanotubes with an outer diameter 20–25 nm and length of 5–15 nm were purchased from Research Institute of Petroleum Industry (RIPI), Tehran, Iran. The synthesis of MMWCNT Nano composite was achieved according to the literature previously reported with some modification [33]. Typically, MWCNTs were first dispersed in concentrated nitric acid at 60℃ for 12 h under stirring to remove the impurities and then washed by copious water and ethanol subsequently. After cleaning, MWCNTs were dried at 110℃ for 4 h. Subsequently, an amount of 0.25 g of purified MWCNTs was suspended in 100 mL of mixed solution containing 0.425 g of ammonium ferrous sulfate and 0.6275 g of ammonium ferric sulfate followed by the slow addition of 2.5 mL of 8 mol/L NH_4OH solution at constant temperature of 50℃ under nitrogen atmosphere with the aid of ultrasonic stirring for 10 min. The pH of the final mixture was controlled in the range of 10–11. The reaction was allowed to be continued for 30 min, which resulted in the suspension changing from black to a brown color. After the completion of the reaction, the suspension was allowed to cool at room temperature. The MMWCNTs were isolated from the mixture by a permanent magnet and dried under vacuum.

2.3 Batch Adsorption Studies

The adsorption experiments were carried out using a series of 200 mL flasks containing 20 mg MMWCNTs and 100 mL 100.0 mg/L AMO solution. The pH of the solutions was adjusted at 7.0 by adding 0.1 M HCl or 0.1 M NaOH solution. After stirring at a 180 rpm for 90 min, the solid/liquid phases were separated by centrifuging at 3600 rpm for 10 min. The residues concentration of AMO was measured using a HPLC (C18 ODS column) with a UV detector 2006 at a wavelength of 190 nm. The mobile phase was a mixture of buffer phosphate with pH= 4.8 and acetonitrile with a volumetric ratio of 60/40 with an injection flow rate of 1 mL/min. The retention time of AMO was 6.5 min. The efficiency (R) and adsorption capacity (q_e) were calculated by equations 1 and 2, respectively [34,35]:

$$R = \frac{(C_0 - C_e)}{C_0} \times 100 \quad (1)$$

$$q_e = \frac{(C_0 - C_e)V}{M} \times 100 \quad (2)$$

Where C_0 (mg/L) is the initial concentration of AMO solution, C_e (mg/L) is the equilibrium concentration of AMO in aqueous solution, V is the volume of the AMO solution (mL); and M is the weight of adsorbent (g).

3. RESULTS AND DISCUSSION

The morphologies of the synthesized MMWCNT adsorbent were obtained by SEM and TEM (shown in Fig. 2). It was observed that iron oxide nanoparticles were successfully coated on the surface of MWCNTs to form multi-wall carbon nano tube-iron oxide nanocomposites.

3.1 Adsorption Isotherm Studies

The adsorption isotherm is the most important information, which indicates how adsorbate molecules are distributed between the liquid phase and solid phase when the adsorption process reaches equilibrium. This study adopted the Langmuir, Freundlich and Tempkin isotherms to describe equilibrium adsorption. Equation parameters and underlying thermodynamic assumptions of these equilibrium isotherms frequently provide some insights into adsorption mechanisms, surface properties and affinities of the adsorbent. The Langmuir model in linear form is presented by equation 3 [36,37]:

$$\frac{C_e}{q_e} = \frac{C_e}{q_{max}} + \frac{1}{q_{max}\, K_L} \quad (3)$$

Where q_e is the amount of AMO adsorbed per gram of MMWNTs (mg/g); C_e is the equilibrium concentration of AMO in a solution (mg/L); K_L is the Langmuir constant (L/mg), which is related

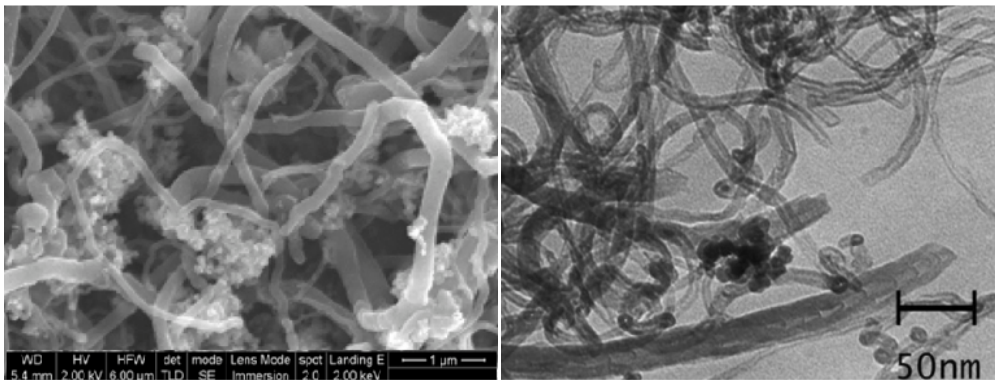

Fig. 2. TEM and SEM images of MMWNTs

to the affinity of binding sites; and q_m is the theoretical saturation capacity of the monolayer (mg/g). The values of q_m and K_L are derived from the intercept and slope of the linear plot of $1/q_e$ versus $1/C_e$.

The Freundlich model in linear form is presented by equation 4 [38,39]:

$$Ln\ q_e = ln\ K_F + \frac{1}{n} ln\ C_e \quad (4)$$

Where q_e and *Ce* are defined as for the Langmuir isotherm and K_F and n are Freundlich constants, which represent adsorption capacity and adsorption strength, respectively. Both K_F and *1/n* can be obtained from the intercept and slope of the linear plot of ln q_e versus ln C_e. The magnitude of 1/n quantifies the favorability of adsorption and the degree of heterogeneity on the surface of MMWNTs. If *1/n* is less than 1, suggesting favorable adsorption capacity increases and new adsorption sites form.

The Tempkin isotherm describes the behavior of adsorption systems on a heterogeneous surface, and is represented by equation 5 [40,41]:

$$q_e = \frac{RT}{b} ln\ (K_t\ C_e) \quad (5)$$

Equation can be expressed in a linear form as [42]:

$$q_e = B_1\ ln\ (K_t) + B\ ln\ (C_e) \quad (6)$$

Where $B_1=\frac{RT}{b}$, and B is a constant related to adsorption heat, and K_t is the equilibrium binding constant (L/mol) corresponding to maximum binding energy. *A* plot of q_e versus ln *Ce* is used to determine isotherm constants.

Table 1 shows the isotherm parameters at different temperatures. Based on the correlation coefficient (R^2) (Table 1), the adsorption of AMO is best fit by the Langmuir isotherm (Fig 3). Notably, K_L, K_F, B_1, n and q_m increased as temperature increased, suggesting that the adsorption of AMO on MMWNTs increased as temperature increased (Table 1). These experimental results reveal that the affinity of binding sites for AMO increased as temperature increased. Since 1/n is less than unity, the adsorption of AMO onto MMWNTs was favored.

3.2 Kinetic Studies

Adsorption is a physicochemical process that involves mass transfer of a solute from liquid phase to the adsorbent surface. Three of the most widely used kinetic models, i.e. Lagergren-first-order equation, pseudo-second-order equation and intra-particle diffusion model were used to research the adsorption kinetic behavior of AMO onto MMWCNTs. The best-fit model was selected based on the linear regression correlation coefficient values (R^2).

Lagergren-first-order kinetic model might be represented by equation 7 [43, 44].

$$Log\ (q_e - q_t) = log\ q_e - \frac{K_1}{2.303} t \quad (7)$$

Where q_e and q_t (mg/g) are the amounts of AMO adsorbed (mg/g) at equilibrium and time t (min), respectively, and k_1 (min^{-1}) is the rate constant of the pseudo-first-order. The parameters k_1 and q_e could be calculated from the slope and intercept of the plots of log (q_e-q_t) versus t and are given in Fig 4. The values of the correlation coefficient R^2 obtained at all the studied concentrations are low, in the range 0.844-0.892. Furthermore, the

experimental values of $q_{e,exp}$ (mg/g) are far from the calculated q_e, cal (mg/g). This suggests that the pseudo-first-order kinetic model is not suitable to describe the adsorption process.

A linear form of pseudo-second-order kinetic model was expressed by equation 8 [45,46]:

$$\frac{t}{q_t} = \frac{1}{K_2 qe^2} + \frac{t}{qe} \quad (8)$$

Where K_2 is the rate constant (g/mg min) of pseudo-second-order kinetic model for adsorption. The slope and intercept of the linear plots of t/q_t against t yield the values of $1/q_e$ and $1/k_2 q_e^2$ for in the equation 8.

Since neither the pseudo first-order nor the second-order model can identify the diffusion mechanism, an intra-particle mass transfer diffusion model proposed by Weber and Morris can be written as follows [47,48]:

$$q_t = K\, t^{0.5} + c \quad (9)$$

Where c (mg/g) is the intercept and K is the intra-particle diffusion rate constant (mg/g min), which can be calculated from the slope of the linear plots of q_t versus $t^{1/2}$.

Different kinetic parameters of AMO adsorption onto MMWCNTs for different AMO initial concentrations are shown in Table 2. All the experimental data showed better compliance with pseudo-second-order kinetic model in terms of higher correlation coefficient values (R^2>0.995). Plots of pseudo-second-order

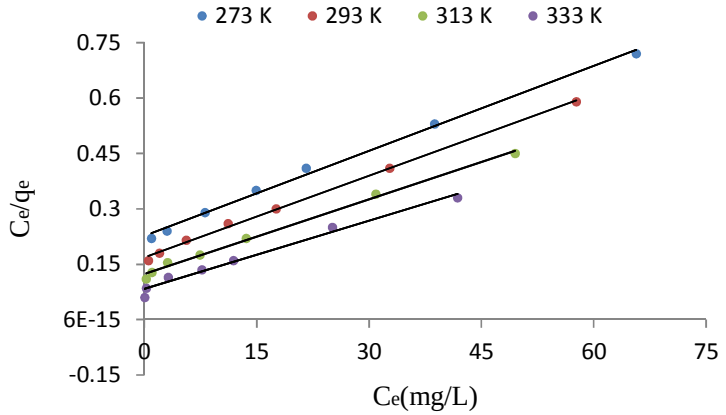

Fig. 3. Langmuir isotherms plots for AMO adsorption on MMWCNTs at various temperatures

Table 1. Isotherm parameters for AMO adsorption onto MMWCNTs

Tem (K)	273	293	313	333
Langmuir				
q_{max}(mg/g)	335.25	355.85	376.25	395.5
K_L (L/mg)	0.1180.0	0.248	0.467	0.565
R_L	781	0.0378	0.0209	0.0173
R^2	0.998	0.999	0.997	0.996
Freundlich				
K_F (mg/g)	7.86	13.52	17.41	20.36
n	1.951	2.41	3.127	6.94
R^2	0.951	0.947	0.916	0.928
Tempkin				
A (L/g)	0.465	0.641	0.795	0.922
B	12.25	10.41	8.172	31.66
R^2	0.795	0.774	0.832	0.814

kinetic models are shown in Fig. 5 for the effect of initial AMO concentrations. It could be found that pseudo-second-order kinetic model was more valid to describe the adsorption behavior of AMO onto MMWCNTs.

The removal of AMO by adsorption on MMWCNTs was found to be rapid at the initial period and then to become slow and stagnate with the increase in contact time.

Typically, various mechanisms control the adsorption kinetics; the most limiting were the diffusion mechanisms, including external diffusion, boundary layer diffusion and intra-particle diffusion. Hence, the intra-particle diffusion model was utilized to determine the rate-limiting step of the adsorption process. If the regression of q_t versus $t^{1/2}$ was linear and passes through the origin, then intraparticle diffusion was the sole rate-limiting step. The regression was linear, but the plot did not pass through the origin (Fig. 6), suggesting that adsorption involved intra-particle diffusion, but that was not the only rate-controlling step. The values of *C* were helpful in determining the boundary thickness: a larger *C* value corresponded to a greater boundary layer diffusion effect. The *C* values (18.45–30.64 mg/g) increased with the initial concentrations (25–200 mg/L) (Table 2). The results of this study demonstrated increasing the initial concentrations promoted the boundary layer diffusion effect.

3.3 Effect of Temperature on AMO Adsorption and Apparent Thermodynamic Studies

The effect of temperature on AMO adsorption was investigated at (273–333 K). As it can be seen from Fig. 6, the adsorption capacity was increased, when the temperature was increased from 273 to 333 K. Increasing the temperature is known to increase the rate of diffusion of the adsorbate molecules across the external boundary layer and in the internal pores of the adsorbent particle, owing to the decrease in the viscosity of the solution.

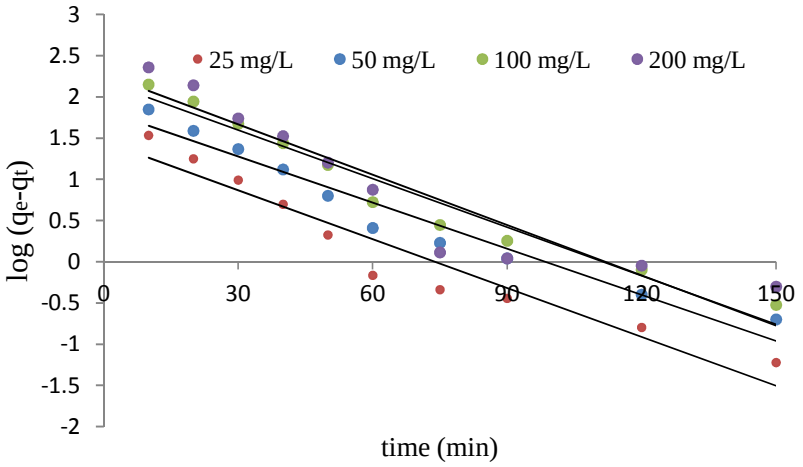

Fig. 4. Pseudo- first order Kinetics for AMO adsorption onto MMWCNTs at different concentration

Table 2. Kinetic parameters for the adsorption of AMO onto MMWCNTs biomass at various concentration

C_o(mg/L)	Pseudo-first order			Pseudo-second order			Intraparticle diffusion		
	K_1	q_e(mg/g)	R^2	K_2	q_e(mg/g)	R^2	K	C	R^2
25	0.0289	48.32	0.892	0.0071	61.24	0.995	0.489	18.45	0.828
50	0.0234	98.41	0.874	0.0058	120.37	0.998	0.614	22.37	0.854
100	0.0158	172.58	0.853	0.0044	218.46	0.999	0.781	27.52	0.861
200	0.0124	310.64	0.844	0.0032	359.25	0.996	0.915	30.64	0.895

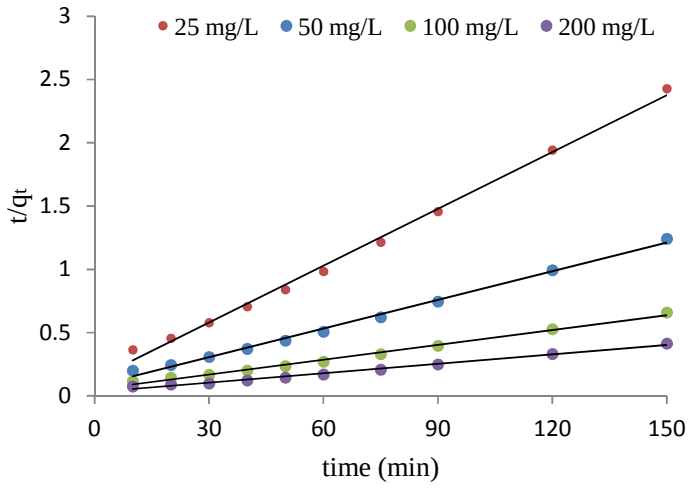

Fig. 5. Pseudo-second order Kinetics for AMO adsorption onto MMWCNTs at different concentration

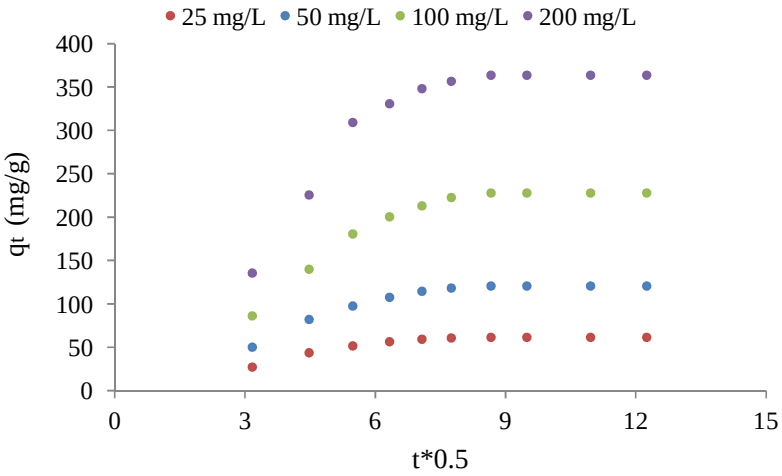

Fig. 6. Intraparticle diffusion Kinetics for AMO adsorption onto MMWCNTs at different concentration

The thermodynamic parameters of Gibb's free energy change, ΔG°, enthalpy change, ΔH°, and entropy change, ΔS°, for the adsorption processes are calculated using the equations 10 and 11 [49,50]:

$$\Delta G^{\circ} = -RT\ Ln\ Ka \quad (10)$$

$$\Delta G^{\circ} = \Delta H^{\circ} - T\Delta S^{\circ} \quad (11)$$

Where R is universal gas constant (8.314 J.mol/K) and T is the absolute temperature in K.

Thermodynamic parameters of AMO adsorption are shown in Table 3. The negative values of ΔG° confirm the feasibility of the process and also the spontaneous nature of adsorption with a high preference of AMO by MMWCNTs. Furthermore, the decrease in the negative value of ΔG° with an increase in temperature indicates that the adsorption process of AMO on MMWCNTs becomes more favorable at higher temperatures.

Adsorption process can be classified as physical adsorption and chemisorptions by the magnitude of the enthalpy change. It is accepted that if magnitude of enthalpy change is lesser than 84 kJ/mol, then the adsorption is physical. However chemisorptions take place in the range of

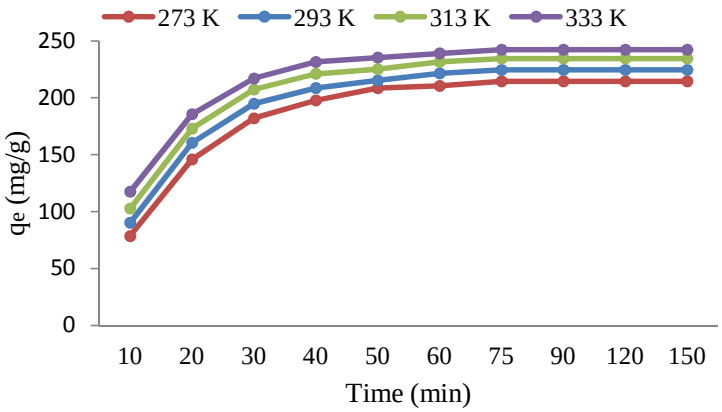

Fig. 7. Effect of temperatures on adsorption capacity (Dose = 0.4 g/L, AMO concentration = 100 mg/L, pH = 7)

Table 3. Thermodynamic parameters of the AMO adsorption on the $MMWCNT_S$ at different temperatures

T (K)	ΔG° (kJ mol^{-1})	ΔS° (J mol^{-1} K^{-1})	ΔH° (kJ mol^{-1})
273	-17.62		
293	-21.44		
313	-25.26	0.191	34.52
333	-29.08		

84–420 kJ/mol. From these results (Table 3 above) it is clear that physisorption is much more favorable for the adsorption of AMO. Also, the positive value of *ΔH°* indicates that the adsorption reaction is endothermic. The positive value of *ΔS°* suggests that some structural changes occur on the adsorbent and the randomness at the solid–liquid interface in the adsorption system increases during the adsorption process [51,52]. Also entropy increase could be due that the separation of the associated-water molecules near to non-polar moieties of the drug after transfer from the solution to the adsorbent [44].

4. CONCLUSIONS

This study investigated the removal of AMO from aqueous solution by MMWCNTs. The adsorption of AMO on MMWCNTs has been described by the Langmuir, Freundlich, Tempkin isotherms. It was found that the data fitted well to Langmuir isotherm (R^2>0.99) better than other isotherms. The adsorption kinetics can be successfully fitted to pseudo-second-order kinetic model. The results of the intra-particle diffusion model suggested that intra-particle diffusion was not the only rate-controlling step. Thermodynamic analyses indicated that the adsorption of AMO onto MMWCNTs was endothermic and spontaneous; Additionally, the adsorption of AMO onto MMWCNTs was via a physisorption process. This study concluded that MMWCNTs are an appropriate adsorbent for removing antibiotics from wastewater.

CONSENT

It is not applicable.

ETHICAL APPROVAL

It is not applicable.

ACKNOWLEDGEMENTS

The authors would like to acknowledge from Qom University of medical sciences for the support this study.

COMPETING INTERESTS

Authors have declared that no competing interests exist.

REFERENCES

1. Chen WR, Huang CH. Adsorption and transformation of tetracycline antibiotics with aluminum oxide. Chemosphere. 2010; 79:779–785.

2. Xu L, Pan J, Dai J, Li X, Hang H, Cao Z, Yan Y. Preparation of thermal-responsive magnetic molecularly imprinted polymers for selective removal of antibiotics from aqueous solution. Journal of Hazardous Materials. 2012;233-234:48-56.
3. Alexy R, Kumpel T, Kummerer K. Assessment of degradation of 18 antibiotics in the closed bottle test. Chemosphere. 2004;57:505–512.
4. Johnson MB, Mehrvar M. Aqueous metronidazole degradation by UV/H_2O_2 process in single-and multi-lamp tubular photoreactors: Kinetics and reactor design, Ind. Eng. Chem. Res. 2008;47:6525–6537.
5. Choi KJ, Kim SG, Kim SH. Removal of antibiotics by coagulation and granular activated carbon filtration. J. Hazard. Mater. 2008;151:38–43.
6. Fatta-Kassinos D, Meric S, Nikolau A. Pharmaceutical residues in environmental waters and wastewater: Current state of knowledge and future research. Anal. Bioanal. Chem. 2011;399:251-275.
7. Zhang W, He G, Gao P, Chen G: Development and characterization of composite nanofiltration membranes and their application in concentration of antibiotics. Sep. Purif. Technol. 2003;30: 27–35.
8. Lanhua Hu L, Flanders PM, Penney L. Miller PL, Timothy J. Strathmann TJ. Oxidation of sulfamethoxazole and related antimicrobial agents by TiO2 photocatalysis. Water Research. 2007; 41(12):2612-26.
9. Yu F, Li Y, Han S, Jie Ma J. Adsorptive removal of antibiotics from aqueous solution using carbon materials. Chemosphere. 2016;153;365–385.
10. Garoma T, Umamaheshwar SH, Mumper A. Removal of sulfadiazine, sulfamethizole, sulfamethoxazole, and sulfathiazole from aqueous solution by ozonation. Chemosphere. 2010;79;814–20.
11. Gulkowsk A, Leung HW, So MK, Taniyasu S, Yamashita N. Removal of antibiotics from wastewater by sewage treatment facilities in Hong Kong and Shenzhen, China. Water research. 2008;42:395-403.
12. Ghauch A, Tuqan A, Assi HA: Elimination of amoxicillin and ampicillin by micro scale and nano scale iron particles. Environ Pollut. 2009;157:1626–1635.
13. Balarak D, Mahdavi Y, Maleki A, Daraei H, Sadeghi S. Studies on the removal of amoxicillin by single walled carbon nanotubes. British Journal of Pharmaceutical Research. 2016;10(4):1-9.
14. Putra EK, Pranowoa R, Sunarsob J, Indraswatia N, Ismadjia S. Performance of activated carbon and bentonite for adsorption of amoxicillin from wastewater: mechanisms, isotherms and kinetics. Water Res. 2009;43:2419-2430.
15. Adrianoa WS, Veredasb V, Santanab CC, Gonçalves LRB. Adsorption of amoxicillin on chitosan beads: Kinetics, equilibrium and validation of finite bath models. Biochemical Engineering Journal. 2005; 27(2):132-37.
16. Balarak D, Mahdavi Y, Mostafapour FK. Application of alumina-coated carbon nanotubes in removal of tetracycline from aqueous solution. British Journal of Pharmaceutical Research. 2016;12(1):1-11.
17. Balarak D, Azarpira H, Mostafapour FK. Study of the adsorption mechanisms of cephalexin on to *Azolla filiculoides*. Der Pharma Chemica. 2016;8(10):114-121.
18. Balarak D, Mostafapour FK, Joghataei A. Experimental and kinetic studies on penicillin G adsorption by *Lemna minor*. British Journal of Pharmaceutical Research. 2016;9(5):1-10.
19. Aksu Z, Tunc O. Application of biosorption for penicillin G removal: Comparison with activated carbon. Process Biochemistry. 2005;40(2):831-47.
20. Ji L, Chen W, Duan L, Zhu D. Mechanisms for strong adsorption of tetracycline to carbon nanotubes: A comparative study using activated carbon and graphite as adsorbents. Environ. Sci. Technol. 2009;43(7):2322–27.
21. Gao J, Pedersen JA. Adsorption of sulfonamide antimicrobial agents to clay minerals. Environ. Sci. Technol. 2005; 39(24):9509-16.
22. Dutta M, Dutta NN, Bhattachary KG. Aqueous phase adsorption of certain beta-lactam antibiotics onto polymeric resins and activated carbon. Separation and Purification Technology. 1999;16(3):213-24.
23. Peterson JW, Petrasky LJ, Seymourc MD, Burkharta RS, Schuilinga AB. Adsorption and breakdown of penicillin antibiotic in the presence of titanium oxide nanoparticles in water. Chemosphere. 2012;87(8):911–7.
24. Balarak D, Mostafapour FK. Canola residual as a biosorbent for antibiotic metronidazole removal. The

Pharmaceutical and Chemical Journal. 2016;3(2):12-17.
25. Malakootian M, Balarak D, Mahdavi Y, Sadeghi SH, Amirmahani N. Removal of antibiotics from wastewater by azollafiliculoides: Kinetic and equilibrium studies. International Journal of Analytical, Pharmaceutical and Biomedical Sciences. 2015;4(7);105-113.
26. Erşan M, Bağd E. Investigation of kinetic and thermodynamic characteristics of removal of tetracycline with sponge like, tannin based cryogels. Colloids and surfaces B: Biointerfaces. 2013;104;75-82.
27. Banerjee SS, Chen DH. Fast removal of copper ions by gum Arabic modified magnetic nano-adsorbent. J. Hazard Mater. 2007;147;792–799.
28. Qu S, Wang J, Kong J, Yang P, Chen G. Magnetic loading of carbon nanotube / nano-Fe_3O_4 composite for electrochemical sensing. Talanta. 2007;71:1096–102.
29. Wu C, Adsorption of reactive dye onto carbon nanotubes: Equilibrium, kinetics and thermodynamics. J. Hazard Mater. 2007;144:93–100.
30. Chung WH. Adsorption of reactive dye onto carbon nanotubes: Equilibrium, kinetics and thermodynamics. J. Hazard Mater. 2007;144:93–100.
31. Ngomsik AF, Bee A, Draye M, Cote G, Cabuil V. Magnetic nano- and microparticles for metal removal and environmental applications: A review. C. R. Chimie. 2005;8:963–70.
32. Ngomsik AF, Bee A, Cote G. Nickel adsorption by magnetic alginate microcapsules containing an extractant. Water Res. 2006;40:1848–56.
33. Ma W, Ya FQ, Han M, Wang R. Characteristics of equilibrium, kinetics studies for adsorption of fluoride on magnetic-chitosan particle. J. Hazard Mater. 2007;143:296–302.
34. Yang N, Zhu S, Zhang D, Xu S. Synthesis and properties of magnetic Fe_3O_4-activated carbon nanocomposite particles for dye removal. Mater. Lett. 2008;62: 645–47.
35. Zazouli MA, Mahvi AH, Dobaradaran S, Barafrashtehpour M, Mahdavi Y, Balarak D. Adsorption of fluoride from aqueous solution by modified *Azolla filiculoides*. Fluoride. 2014;47(4):349-58.
36. Diyanati RA, Yousefi Z, Cherati JY, Balarak D. The ability of Azolla and *Lemna minor* biomass for adsorption of phenol from aqueous solutions. J Mazand Uni Med Sci. 2013;23(106):17-23.
37. Zazouli MA, Yazdani J, Balarak D, Ebrahimi M, Mahdavi Y. Removal acid blue 113 from aqueous solution by canola. J Mazand Uni Med Sci. 2013;23(2):73-81.
39. Chang PH, Li Z, Jean JS, Jiang WT, Wang CJ, Lin KH. Adsorption of tetracycline on 2:1 layered non-swelling clay mineral illite. Appl. Clay Sci. 2012;67:158–163.
40. Diyanati RA, Yousefi Z, Cherati JY, Balarak D. Adsorption of phenol by modified Azolla from aqueous solution. J Mazand Uni Med Sci. 2013;22(2): 13-21.
41. Balarak D, Mostafapour FK, Joghataei A. Adsorption of Acid Blue 225 dye by multi walled carbon nanotubes: Determination of equilibrium and kinetics parameters. Der Pharma Chemica. 2016;8(8):138-145.
42. Upadhyayula VKK, Deng S, Mitchell MC, Smith GF. Application of carbon nanotube technology for removal of contaminants in drinking water: A review. Science of the Total Environment. 2009;408:1–13.
43. Balarak D, Joghataei A. Biosorption of Phenol using dried Rice husk biomass: Kinetic and equilibrium studies. Der Pharma Chemica. 2016;8(6):96-103.
44. Balarak D, Jaafari J, Hassani G, Mahdavi Y, Tyagi I, Agarwal S, Gupta VK. The use of low-cost adsorbent (Canola residues) for the adsorption of methylene blue from aqueous solution: Isotherm, kinetic and thermodynamic studies. Colloids and Interface Science Communications. 2015; 7:16–19.
45. Rostamian R, Behnejad H. A comparative adsorption study of sulfamethoxazole onto graphene and graphene oxide nanosheets through equilibrium, kinetic and thermodynamic modeling. Process Safety and Environmental Protection. 2016;102: 20-29.
46. Balarak D, Mahdavi Y, Bazrafshan E, Mahvi AH, Esfandyari Y. Adsorption of fluoride from aqueous solutions by carbon nanotubes: Determination of equilibrium, kinetic and thermodynamic parameters. Flouride. 2016;49(1):35-42.
47. Balarak D, Mahdavi Y, Bazrafshan E, Mahvi AH. Kinetic, isotherms and thermodynamic modeling for adsorption of acid blue 92 from aqueous solution by modified *Azolla filicoloides.* Fresenius Environmental Bulletin. 2016;25(5): 1321-30.

48. Zazouli MA, Mahvi AH, Mahdavi Y, Balarakd D. Isothermic and kinetic modeling of fluoride removal from water by means of the natural biosorbents sorghum and canola. Fluoride. 2015;48(1):15-22.
49. Balarak D. Kinetics, Isotherm and thermodynamics studies on bisphenol A Adsorption using Barley husk. International Journal of Chem Tech Research. 2016; 9(5):681-690.
50. Balarak D, Azarpira H, Mostafapour FK. Thermodynamics of removal of cadmium by adsorption on Barley husk biomass. Der Pharma Chemica. 2016;8(10): 243-247.
51. Khaled A, Nem AE, El-Sikaily A, Abdelwahab O. Removal of direct N blue-106 from artificial textile dye effluent using activated carbon from orange peel: Adsorption isotherm and kinetic studies. J. Hazard. Mater. 2009;165:100–110.
52. Gao Y, Li Y, Zhang L, Huang H, Hu J, Shah SM, Su X. Adsorption and removal of tetracycline antibiotics from aqueous solution by graphene oxide. J. Colloid. Interface Sci. 2012;368:540–546.

Peer-review history:
The peer review history for this paper can be accessed here:
http://sciencedomain.org/review-history/19219